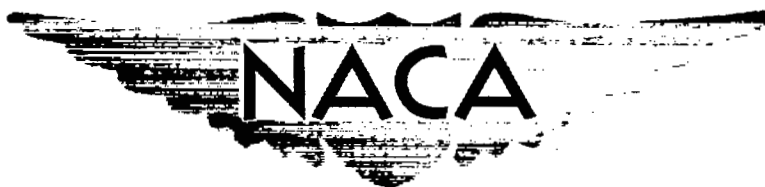


~~RESTRICTED~~
UNCLASSIFIED
SEP 17 1951

0.2



RESEARCH MEMORANDUM

PERFORMANCE OF SINGLE-STAGE COMPRESSOR DESIGNED ON
BASIS OF CONSTANT TOTAL ENTHALPY WITH SYMMETRICAL
VELOCITY DIAGRAM AT ALL RADII AND VELOCITY RATIO
OF 0.7 AT ROTOR HUB

By Jack R. Burt and Robert J. Jackson

~~CLASSIFICATION CANCELLED~~ Lewis Flight Propulsion Laboratory
Cleveland, Ohio

Authority J. W. Cronley Date 12/14/53

By W. J. A. 1/11/54 See NACA

CLASSIFIED DOCUMENT

This document contains classified information affecting the National Defense of the United States within the meaning of the Espionage Act, USC 5031 and 32. Its transmission or the revelation of its contents in any manner to an unauthorized person is prohibited by law.
Information so classified may be imparted only to persons in the military and naval services of the United States, appropriate civilian officers and employees of the Federal Government who have a legitimate interest therein, and to United States citizens of known loyalty and discretion who of necessity must be informed thereof.

NATIONAL ADVISORY COMMITTEE FOR AERONAUTICS

WASHINGTON

September 6, 1951

LIBRARY

LEWIS FLIGHT PROPULSION LABORATORY

CLEVELAND, OHIO

~~RESTRICTED~~
UNCLASSIFIED

UNCLASSIFIED

1
NACA RM E51F06

NATIONAL ADVISORY COMMITTEE FOR AERONAUTICS

RESEARCH MEMORANDUM

PERFORMANCE OF SINGLE-STAGE COMPRESSOR DESIGNED ON BASIS OF
CONSTANT TOTAL ENTHALPY WITH SYMMETRICAL VELOCITY DIAGRAM

AT ALL RADII AND VELOCITY RATIO OF 0.7 AT ROTOR HUB

By Jack R. Burt and Robert J. Jackson

SUMMARY

The results of an investigation of the over-all and stage-element performance of a single-stage compressor designed for a ratio of inlet axial velocity at the rotor hub to tip speed of 0.7 are presented over a range of speeds up to 130-percent design speed.

The stage, consisting of 19 rotor blades and 20 stator blades with 40 inlet guide vanes, had a hub-to-tip radius ratio at the rotor inlet of 0.50 and a rotor tip diameter of 14 inches. The rotor and stator blades were of constant chord from hub to tip and had a modified NACA 65-(12)10 profile.

A peak pressure ratio of 1.22 was obtained at the design tip speed (938 ft/sec) at an equivalent weight flow of 24.0 pounds per second and an efficiency of 0.87. At 120-percent design speed (tip speed, 1126 ft/sec), a peak pressure ratio of 1.28 was obtained at an efficiency of 0.76 and an equivalent weight flow of 27 pounds per second. For a pressure ratio of 1.21 at a tip speed of 1126 feet per second, an equivalent weight flow of approximately 30 pounds per second was obtained at an efficiency of 78 percent. This flow corresponds to 28 pounds per second per square foot of frontal area. Beyond a tip speed of 1126 feet per second, the efficiency dropped sharply and very little gain was realized in either pressure ratio or weight flow.

The effect of Mach number on peak stage-element efficiency is presented over a range of rotor relative inlet Mach numbers from approximately 0.5 to 0.875. The data indicate that a Mach number of about 0.8 is the critical value for all the stage elements since efficiency decreased rapidly beyond this Mach number.

INTRODUCTION

The results reported herein are from part of an investigation of typical axial-flow compressor inlet stages being conducted at the NACA Lewis laboratory. An analysis of the effects of basic design variables (reference 1) indicates that the use of a constant-total-enthalpy design

UNCLASSIFIED

having symmetrical velocity diagrams at all radii would provide a good compromise of pressure ratio, mass flow, and tip speed. This flow distribution was therefore used throughout the present investigation. The first design investigated had a design ratio of axial velocity to tip speed of 0.6 upstream of the rotor at the hub (reference 2). The performance was characterized by high pressure ratio and tip speed.

The data reported herein are from a design having a ratio of axial velocity at the rotor hub to tip speed of 0.7, which resulted in reduced wheel speed and pressure ratio but in increased mass flow.

The compressor, which is completely described in reference 2, had a rotor tip diameter of 14 inches and a hub-to-tip radius ratio of 0.5 at the rotor inlet. The blading consisted of 19 rotor blades, 20 stator blades, and 40 sheet-metal circular-arc guide vanes that provided the required prerotation. The rotor and stator blades were of constant chord and had a modified NACA 65-(12)10 compressor-blade profile.

The performance of the compressor was investigated at equivalent tip speeds of 469, 704, 938, 1126, and 1219 feet per second corresponding to 50-, 75-, 100-, 120-, and 130-percent design speed, respectively. This speed range corresponds to rotor relative inlet Mach numbers of approximately 0.5 to 0.875. Flow measurements were made upstream of the rotor blades and downstream of the stator blades for full-stage performance. Over-all performance is presented in terms of adiabatic temperature-rise efficiency and total-pressure ratio over a weight-flow range at each speed. Details of stage-element performance are given by plots of element efficiency, pressure ratio, and angles of attack against weight flow at design and 120-percent design speeds. Temperature-rise energy addition is plotted against radius for the range of weight flow at design speed. The effects of Mach number on peak element efficiencies and the angles of attack corresponding to these efficiencies are presented.

SYMBOLS

The following symbols are used in this report:

C_L	lift coefficient
ΔH	total enthalpy rise, (ft-lb/slug)
K	constant in turning-angle relation
r	radius to blade element, (ft)
u	velocity of blade at radius r , (ft/sec)

V	absolute air velocity, (ft/sec)
V'	air velocity relative to rotor, (ft/sec)
W	weight flow, (lb/sec)
$\frac{W\sqrt{\theta}}{\delta}$	weight flow corrected to standard sea-level pressure and temperature, (lb/sec)
α	angle of attack, (deg)
$\alpha_{i,0}$	angle of attack of isolated airfoil for zero lift, (deg)
β	absolute stagger angle, angle between compressor axis and absolute air velocity, (deg)
β'	relative stagger angle, angle between compressor axis and air velocity relative to rotor, (deg)
$\Delta\beta'$	relative turning angle in rotor, (deg)
δ	ratio of inlet total pressure to standard sea-level pressure
θ	ratio of inlet total temperature to standard sea-level temperature
σ	blade-element solidity, ratio of chord length to distance between adjacent blades
Φ	blade-angle setting, (deg)
Subscript:	
t	tip

COMPRESSOR DESIGN

Mechanically, the subject compressor is identical to the compressor reported in reference 2. The stage, consisting of 19 rotor blades and 20 stator blades with 40 inlet guide vanes, had a hub-to-tip radius ratio at the rotor inlet of 0.50 and a rotor-tip diameter of 14 inches. Aerodynamically, the design is similar to that of reference 2 (based on constant total enthalpy and symmetrical velocity diagram at all radii). The design differed from reference 2 only in the values for the ratio of axial velocity at the rotor hub to tip speed and the limiting rotor relative inlet Mach number at the hub. Both of these values were assumed to be 0.7 for the design reported herein. Briefly the design procedure was as follows:

Axial velocity was assumed constant within a blade row at any given radius and a limiting value of σC_L of 0.77 was used for the rotor. From inlet Mach number and σC_L limitations at the hub, axial and tangential velocity components were calculated for an assumed flow parallel to the compressor axis through an untapered passage having a symmetrical velocity diagram. The density ratio over the stage was computed for an assumed vortex-whirl addition in the rotor and an efficiency of 0.89. Passage taper was determined from continuity and velocities were corrected assuming uniform streamline flow. Blade-angle settings, however, were computed by using the velocities previously calculated for flow parallel to the axis. Simple radial equilibrium was assumed at the rotor inlet but was neglected between the rotor and stator blade rows.

The blade-angle settings were calculated from the Kantrowitz and Daum equation (reference 3):

$$\Delta\beta' = K(\alpha - \alpha_{1,0})$$

with $K = 0.9$ as described in reference 2. These settings were modified near the tip for the low solidities encountered but to a lesser extent than in reference 2 because of lower stagger angles. The calculated blade setting at the tip was modified by an arbitrary reduction of $2\frac{1}{2}^\circ$ and by fairing in the modification to a radius ratio of about 0.8.

A modified NACA 65-(12)10 profile with constant chord from hub to tip was used for the blading. The radial variation of blade-design data such as angle settings Φ , solidity σ , and entering air angle β are presented in figure 1.

APPARATUS AND PROCEDURE

The compressor installation and instrumentation are similar schematically to those described in reference 2. In order to permit higher speeds and weight flows, however, a 1500-horsepower motor and a new exhaust system were incorporated. Also, the instrumentation technique was refined to permit measurements of the state of the air downstream of the stationary blades in regions where there were no blade wakes.

Flow measurements were taken approximately 0.2 chord length upstream of the rotor blades and 0.6 chord length downstream of the stator blades. Data were taken at five radial stations a, b, c, d, and e from tip to hub, which were located at the centers of five equal spaces across the passage upstream of the rotor blades and downstream of the stator blades. The investigation was conducted at constant values of equivalent rotor tip speed $U_t/\sqrt{\theta}$ of 469, 704, 938, 1126, and 1219 feet per second corresponding to 50-, 75-, 100-, 120-, and 130-percent design speed, respectively. At each speed, a range of air

flow was investigated from either the highest flow possible or that flow at which there was no pressure rise over the tip of the blade to a low flow at which the blades stalled near the tip.

RESULTS AND DISCUSSION

Over-all Compressor Performance

The over-all performance characteristics of the compressor are presented in figure 2 in terms of adiabatic temperature-rise efficiency and total-pressure ratio as functions of weight flow corrected to sea-level conditions. At the design tip speed, 938 feet per second, a peak pressure ratio of 1.22 was obtained at an efficiency of 0.87 and a corrected weight flow of 24 pounds per second. A peak efficiency of 0.88 was obtained at a corrected weight flow of 24.5 pounds per second with a total-pressure ratio of 1.21.

At 120-percent design speed (tip speed, 1126 ft/sec) the inlet relative Mach number was approximately 0.80 at the mean radius. A peak pressure ratio of 1.28 was obtained at an efficiency of 0.76 and an equivalent weight flow of 27 pounds per second. At a pressure ratio of 1.21, which corresponds to the peak efficiency point at design speed, a weight flow of approximately 30 pounds per second (28 lb/sec/sq ft frontal area) was obtained at an efficiency of 0.78. This flow is 75.7 percent of the limiting flow at sonic axial velocity for the compressor unit. The peak efficiency dropped sharply beyond this tip speed of 1126 feet per second and very little gain was obtained in either pressure ratio or weight flow. At 130-percent design speed (tip speed, 1219 ft/sec), peak efficiency, peak pressure ratio, and maximum weight flow were 0.70, 1.30, and 30.9 pounds per second, respectively.

Stage-Element Performance Characteristics

In order to compare stage-element performance characteristics, a particle of air is assumed to travel a path through the stage which connects the five measuring stations at the rotor inlet to the five similarly located measuring stations at the stator outlet. One such path is then, by definition, a stage element. Adiabatic temperature-rise efficiencies, total-pressure ratios, and angles of attack at the five measuring stations are presented as functions of corrected weight flow for design speed and 120-percent design speed in figure 3.

At design speed (fig. 3(a)) the stage elements appear to be well matched in that the efficiencies all peak at approximately the same weight flow. Maximum efficiencies at the measuring stations near the hub and the tip of the stage are lower because of wall boundary-layer and secondary flow effects. Near the tip where stagger angles are 50° to 60° and solidity is approximately 0.6, the range of angle of attack for good efficiency is small and the efficiencies peak rapidly. Near the hub where the range of stagger angle is 30° to 40° and the solidity is near 1.0, a greater range of angle of attack for good efficiency is available and the efficiencies remain relatively constant over the entire range of weight flow investigated.

At 120-percent design speed (fig. 3(b)) the stage elements are no longer matched; the over-all efficiency is therefore lower. The higher Mach number also causes a general decrease in angle-of-attack range for good efficiency for all stage elements and accentuates the reduction in range and low-efficiency operating conditions obtained because of the solidity and stagger angle combination near the blade tip. The stage-element efficiencies also show that the low efficiencies near the tip of the blade at 120-percent design speed are responsible for a large part of the decrease in over-all stage efficiency.

The angles of attack for both speeds show a slightly greater variation near the tip with weight flow than near the hub. This variation, together with the higher wheel speed at the tip and a small range of optimum angle of attack because of the solidity and stagger angle combination, causes a larger variation in pressure ratio near the tip than at the other stations. The greater change in angle of attack per increment of weight flow near the tip also suggests that the work input will change faster in that region. This trend is shown in figure 4, which is a plot of temperature-rise energy addition against radius for the range in weight flows investigated at design speed. The design criterion of constant total enthalpy is approached only at the highest weight flows. A detailed discussion of the reasons for the variations in enthalpy distribution is presented in reference 2.

Effects of High Mach Number on Stage-Element Efficiency

As the compressor speed was increased, the resulting increase in Mach number caused the matching of the stage elements to change and the peak efficiencies to be reduced. Also, the most critical stage element is near the tip of the blades where stagger angles are high and the solidity is low. The maximum adiabatic temperature-rise efficiencies and the respective angles of attack for the rotor blades plotted against Mach number are presented in figure 5. The critical Mach number for all the stage elements appears to be slightly less than 0.8. However, because of the matching of the stage elements in

this design, the critical value for all stage elements does not occur at any one weight flow. It would probably be desirable, therefore, to operate at a tip speed corresponding to a slightly lower Mach number than the critical value for any of the stage elements. In this design, the element that reached its critical value first was at the blade tip.

For a typical airfoil section, the angle of attack for maximum lift-drag ratio or peak efficiency lies near the high angle of attack end of the low-drag range. The low-drag range is appreciably reduced as the Mach number is increased; it would therefore be expected that the angle of attack for peak efficiency would decrease. In general, this is the trend for the stage reported herein as shown in figure 5. The reason for the indicated increase in angle of attack near the tip of the blades, as shown in figure 5 for the Mach numbers beyond the critical value, is not obvious. However, this phenomenon is of little practical importance because it occurs at Mach numbers beyond the critical Mach number of the stage elements.

SUMMARY OF RESULTS

The results of an investigation of the over-all and stage-element performance of a single-stage compressor designed for a ratio of inlet axial velocity at the rotor hub to tip speed of 0.7 are presented over a range of rotor relative inlet Mach numbers from 0.5 to 0.875.

1. At 120-percent design speed (tip speed, 1126 ft/sec) a peak pressure ratio of 1.28 was reached at a corrected weight flow of 27 pounds per second at an efficiency of 0.76. At a weight flow of 30 pounds per second, a pressure ratio of 1.21 was obtained at an efficiency of 0.78. A flow of 30 pounds per second corresponds to 28 pounds per second per square foot frontal area.

2. The low solidity and high stagger angle combination near the tip of the rotor blade gave a rapidly peaking stage-element efficiency and thus an over-all stage-efficiency curve with only a small range of good efficiency at a given speed. Near the hub the element efficiency was relatively constant over the range of weight flow investigated.

3. Temperature-rise energy addition at a given speed increased from hub to tip, the greatest rate of change occurring near the tip for a given increment of weight flow.

4. In the region of high stagger angles and low solidity near the blade tip, an increase in Mach number decreased the optimum range of angle of attack to the extent that matching of blade elements over a range of Mach numbers was very difficult to obtain for this stage design with a constant-camber blade.

5. A Mach number of slightly less than 0.80 was the critical Mach number for all the stage elements of the design investigated in that the efficiencies decreased rapidly beyond this value.

Lewis Flight Propulsion Laboratory
National Advisory Committee for Aeronautics
Cleveland, Ohio

REFERENCES

1. Sinnette, John T., Jr.: Analysis of Effect of Basic Design Variables on Subsonic Axial-Flow-Compressor Performance. NACA Rep. 901, 1948. (Formerly RM E7D28.)
2. Burt, Jack R.: Investigation of Performance of Typical Inlet Stage of Multistage Axial-Flow Compressor. NACA RM E9E13, 1949.
3. Kantrowitz, Arthur, and Daum, Fred L.: Preliminary Experimental Investigation of Airfoils in Cascade. NACA CB, July 1942.

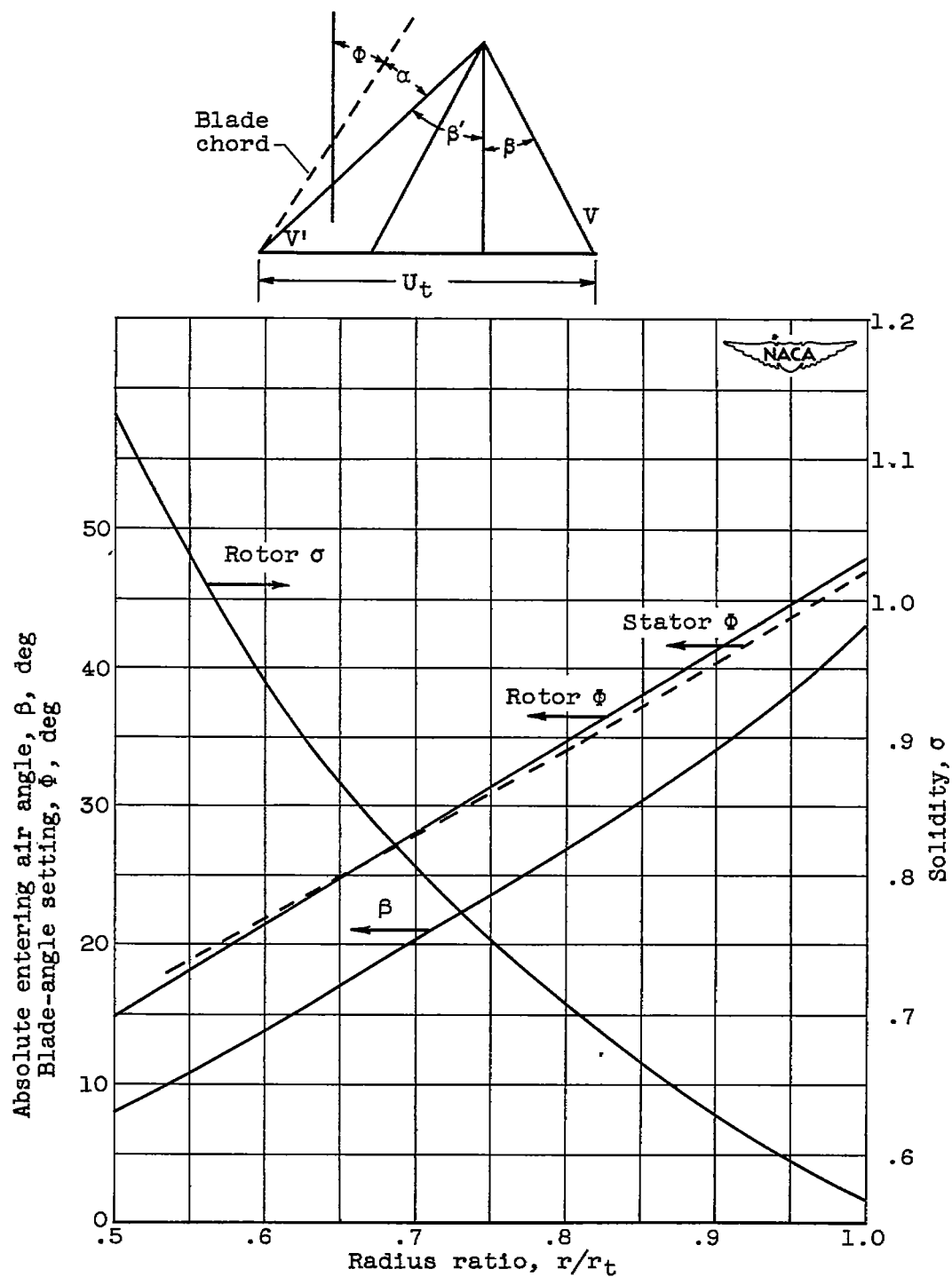


Figure 1. - Blading details for inlet stage with NACA 65-(12)10 blade section.

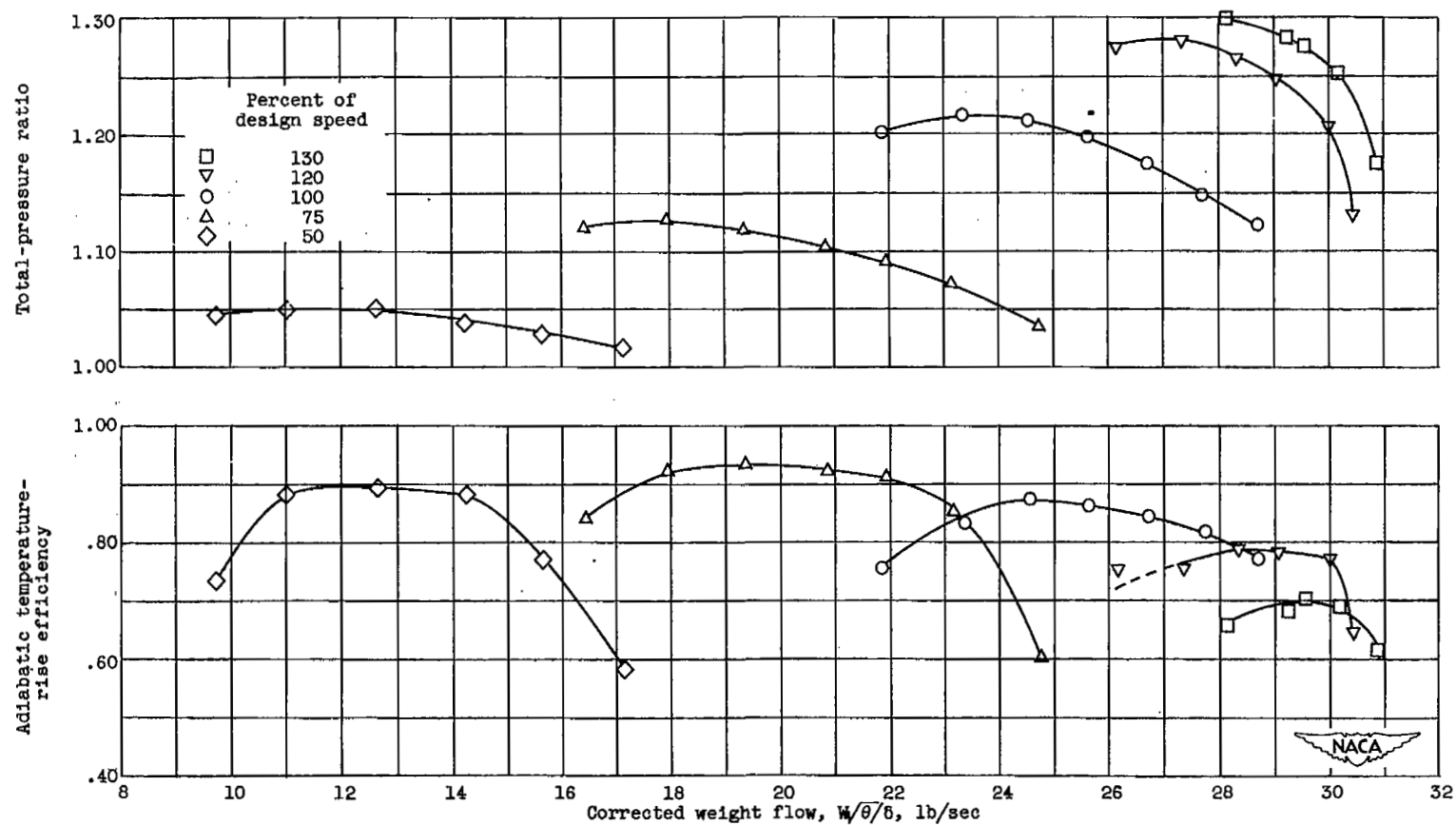
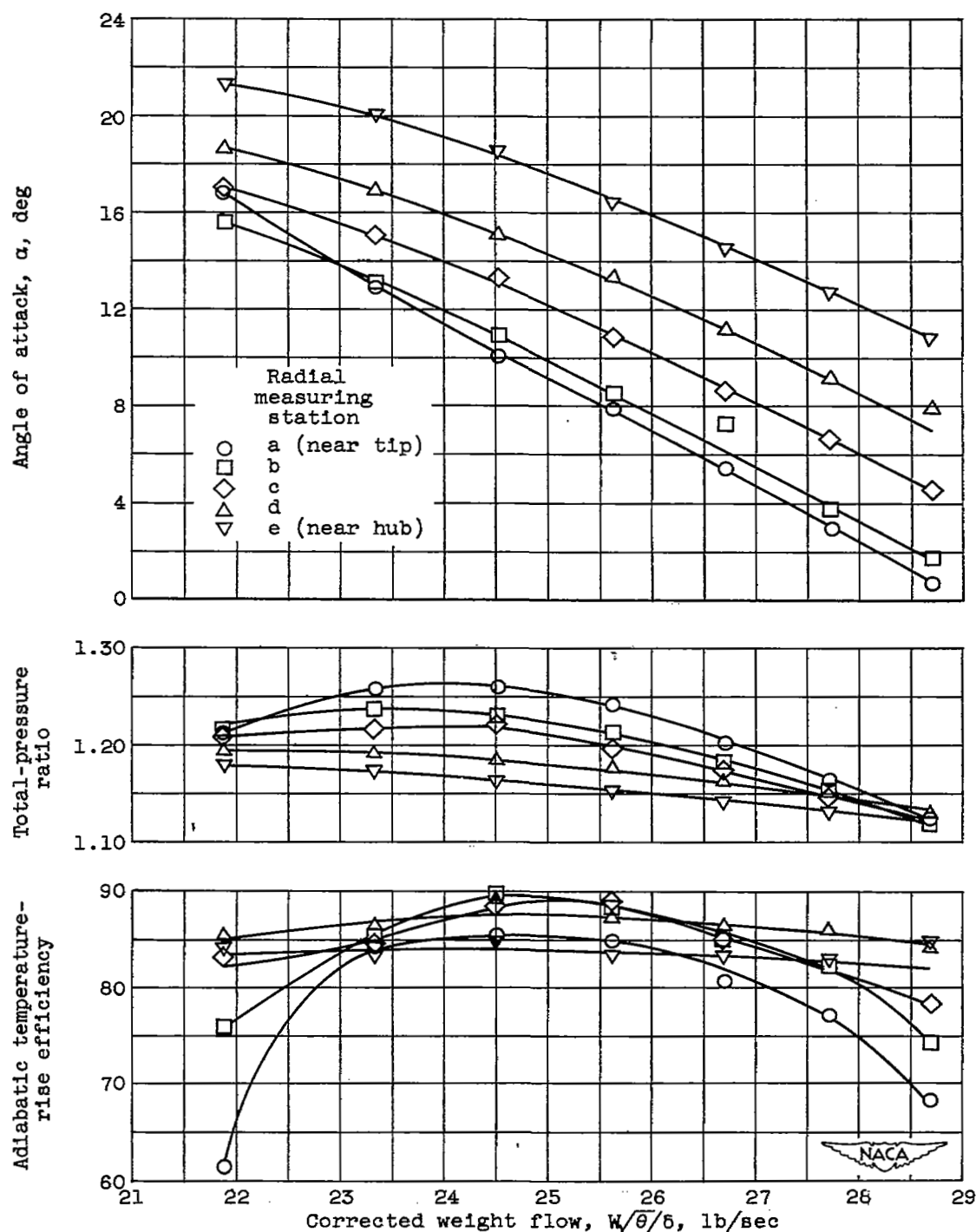
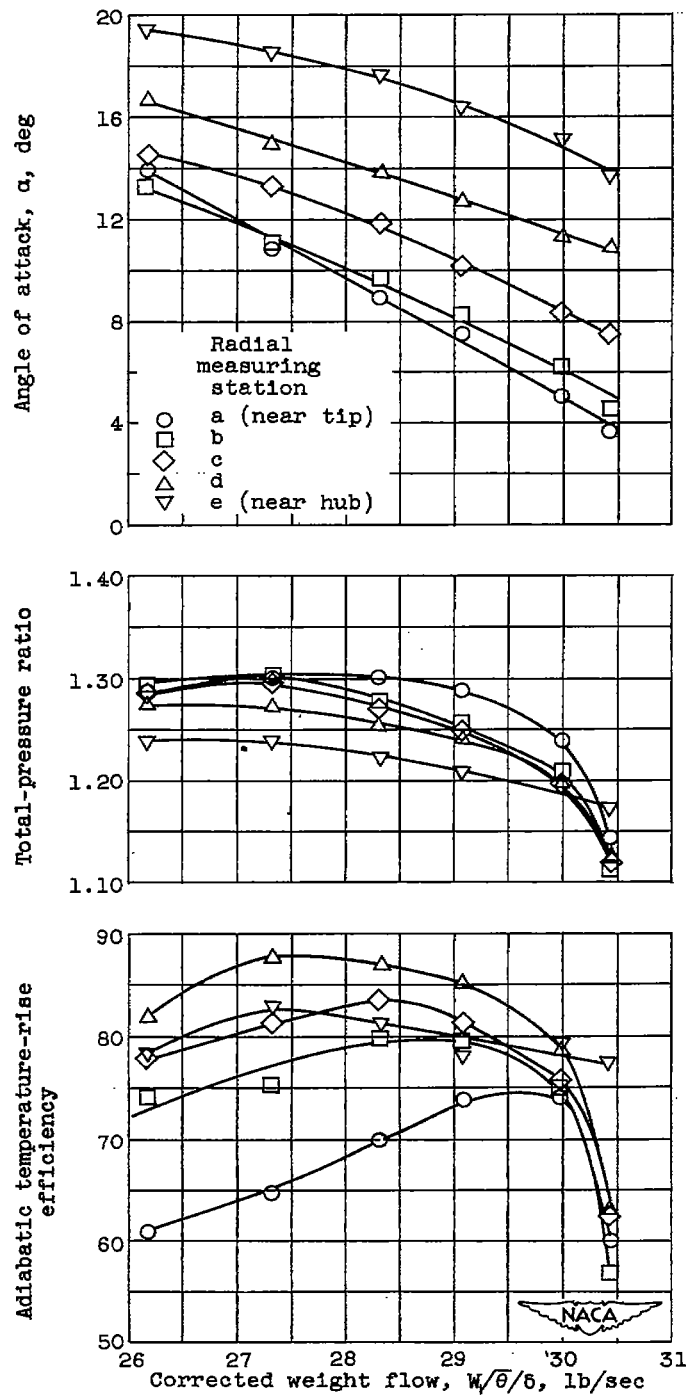


Figure 2. - Over-all performance of inlet stage with NACA 65-(12)10 blade section.



(a) Design speed.

Figure 3. - Stage-element performance characteristics for five radial measuring stations.



(b) 120-percent design speed.

Figure 3. - Concluded. Stage-element performance characteristics for five radial measuring stations.

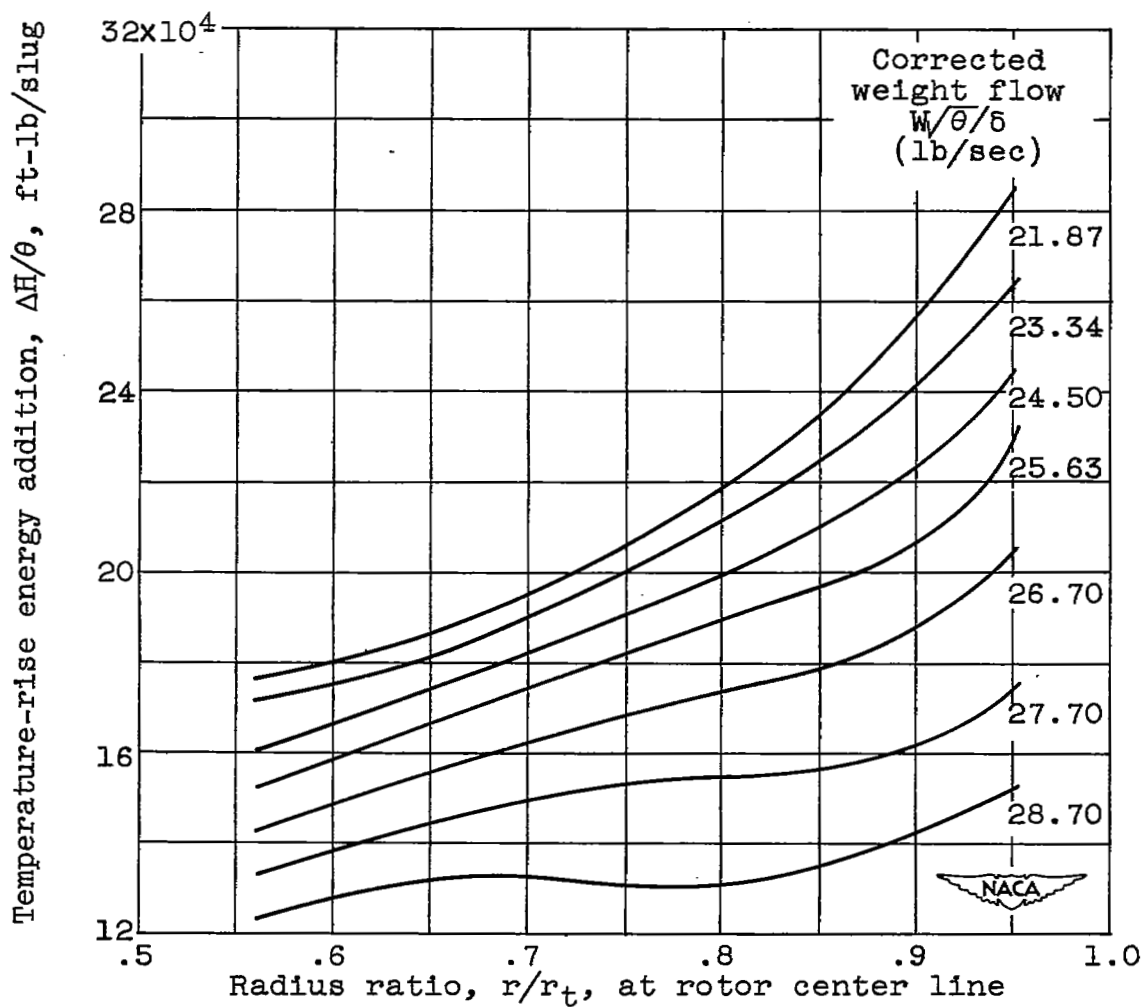


Figure 4. - Energy addition plotted against radius ratio at design speed.

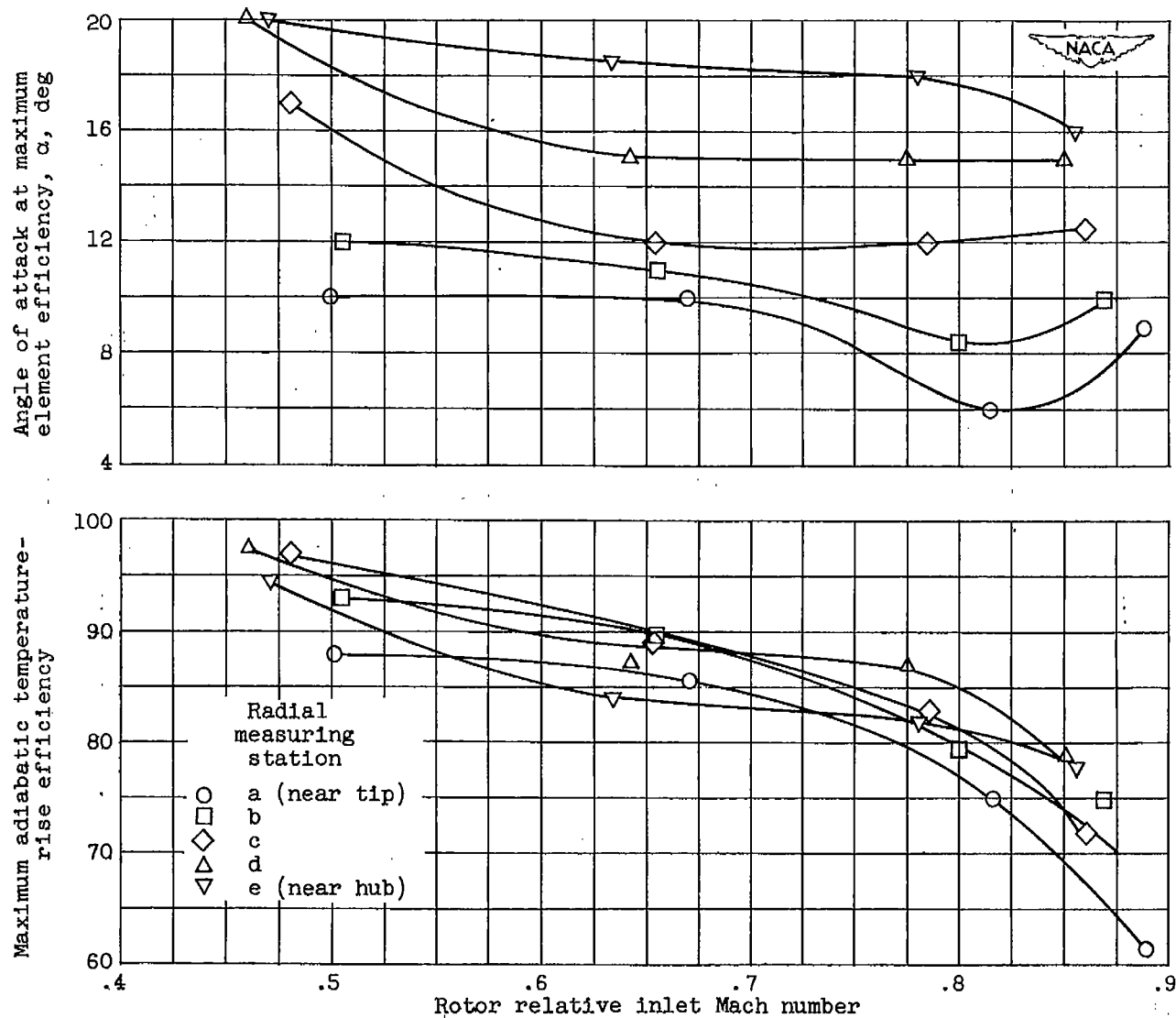


Figure 5. - Effect of Mach number on maximum efficiency.